



Published in final edited form as:

Cell Stem Cell. 2014 July 3; 15(1): 66–78. doi:10.1016/j.stem.2014.03.005.

Hydrogen Sulfide Maintains Mesenchymal Stem Cell Function and Bone Homeostasis *via* Regulation of Ca²⁺ Channel Sulphydration

Yi Liu^{1,2,*}, Ruili Yang¹, Xibao Liu³, Yu Zhou⁴, Cunye Qu¹, Takashi Kikuri¹, Songlin Wang², Ebrahim Zandi⁴, Junbao Du⁵, Indu S. Ambudkar³, and Songtao Shi^{1,*}

¹Center for Craniofacial Molecular Biology, Ostrow School of Dentistry, University of Southern California, 2250 Alcazar Street, CSA 103, Los Angeles, CA 90033, USA

²Department of Periodontics, Capital Medical University School of Stomatology, Tian Tan Xi Li No. 4, Beijing 100050, China

³Molecular Physiology and Therapeutics Branch, National Institute of Dental and Craniofacial Research, Bethesda, MD 20892 USA

⁴Department of Molecular Microbiology and Immunology, University of Southern California, 2011 Zonal Avenue, Los Angeles, CA 90033, USA

⁵Department of Pediatrics, Peking University First Hospital, Beijing 100034, China

SUMMARY

Gaseous signaling molecules such as hydrogen sulfide (H₂S) are produced endogenously and mediate effects through diverse mechanisms. H₂S is one such gasotransmitter which regulates multiple signaling pathways in mammalian cells, and abnormal H₂S metabolism has been linked to defects in bone homeostasis. Here, we demonstrate that bone marrow mesenchymal stem cells (BMMSCs) produce H₂S to regulate their self-renewal and osteogenic differentiation, and H₂S deficiency results in defects in BMMSC differentiation. H₂S deficiency causes aberrant intracellular Ca²⁺ influx, due to reduced sulphydration of cysteine residues on multiple Ca²⁺ TRP channels. This decreased Ca²⁺ flux downregulates PKC/Erk-mediated Wnt/β-catenin signaling which controls osteogenic differentiation of BMMSCs. Consistently, H₂S-deficient mice display an osteoporotic phenotype, which can be rescued by small molecules which release H₂S. These results demonstrate H₂S regulates BMMSCs, and restoring H₂S levels *via* non-toxic donors may provide treatments for diseases such as osteoporosis which can arise from H₂S deficiencies.

© 2014 Il Press. All rights reserved.

*Correspondence: Dr. Songtao Shi, Center for Craniofacial Molecular Biology, University of Southern California, 2250 Alcazar Street, CSA-103, Los Angeles, CA 90033, USA, Tel: 323-442-3038, Fax: 323-442-2981, songtaos@usc.edu Or Dr. Yi Liu, Department of Periodontics, Capital Medical University School of Stomatology, Tian Tan Xi Li No. 4, Beijing 100050, China, Tel: 01186-18600262811, liuyi@ccmu.edu.cn.

SUPPLEMENTAL INFORMATION

Supplemental Information includes 11 figures, 2 tables, and supplementary experimental procedures.

Publisher's Disclaimer: This is a PDF file of an unedited manuscript that has been accepted for publication. As a service to our customers we are providing this early version of the manuscript. The manuscript will undergo copyediting, typesetting, and review of the resulting proof before it is published in its final citable form. Please note that during the production process errors may be discovered which could affect the content, and all legal disclaimers that apply to the journal pertain.

INTRODUCTION

Hydrogen sulfide (H₂S) is a colorless and poisonous gas with the characteristic foul odor of rotten eggs. Recent studies showed that H₂S serves as a gasotransmitter to regulate a variety of signaling pathways (Wang, 2003). Physiologically, H₂S plays an important role in the induction of hippocampal long-term potentiation, brain development, blood pressure regulation and inflammatory responses (Fiorucci et al., 2005; Li et al., 2006; Olson and Donald, 2009; Yusuf et al., 2005; Zhong et al., 2003). Abnormal H₂S metabolism has been linked to several human diseases, including Alzheimer's, hypertension, coronary heart disease, atherosclerosis, cataracts, pancreatitis and type 1 diabetes (Donovan et al., 2011; Gil et al., 2011; Li et al., 2005).

In mammals, H₂S is generated from L-cysteine catalyzed by two pyridoxal-5'-phosphate-dependent enzymes, termed cystathionine β-synthase (CBS) and cystathionine γ-lyase (CSE) (Bukovska et al., 1994; Erickson et al., 1990; Swaroop et al., 1992; Wang, 2002). CBS and CSE expression has been identified in many human and other mammalian cells, including those from liver, kidney, brain, smooth muscle, pancreas and lymphocytes (Stipanuk and Beck, 1982; Tang et al., 2006). CBS is reported to be the predominant H₂S-generating enzyme in the brain and nervous system, and CSE is mainly expressed in the vascular smooth muscles and pancreas (Abe and Kimura, 1996; Bao et al., 1998; Simpson and Freedland, 1976).

CBS deficiency is an autosomal recessive disease that is the most frequent cause of clinical hyperhomocysteinemia and homocystinuria (Uren et al., 1978; Watanabe et al., 1995). Patients may have multisystem disorders, including dislocated lenses, mental deficiency, premature arteriosclerosis, thrombosis, and osteoporosis. Epidemiological and clinical studies suggest that hyperhomocysteinemia patients have an increased risk of fracture (Dhonukshe-Rutten et al., 2005; Gjesdal et al., 2007; McLean et al., 2004; van Meurs et al., 2004). However, the etiology for the increased prevalence of osteoporosis in these patients remains unclear. Although a high serum level of homocysteine (HCY) has been considered as one of the factors causing osteoporosis in these patients, controversial reports on the effects of high levels of HCY on osteoclasts and osteoblasts have made it difficult to uncover the precise mechanism. In addition to elevated HCY, CBS-deficient patients also have notable reduced H₂S level. Therefore, we hypothesize that a stable, low level of H₂S in the human body may play an important role in maintaining the homeostasis of the bone/marrow system.

Bone marrow mesenchymal stem cells (BMMSCs) are nonhematopoietic multipotent stem cells and play an important role in maintenance of the bone/marrow homeostasis (Friedenstein et al., 1974; Pittenger et al., 1999; Prockop, 1997). BMMSCs and BMMSC-derived osteoblasts are responsible for bone formation and balancing osteoclast-mediated bone resorption to maintain bone mineral density. It is unknown whether BMMSCs produce H₂S or if H₂S levels affect BMMSC function. In this study, we show that BMMSCs express both CBS and CSE and produce H₂S. More importantly, H₂S is required to maintain stem cell properties in BMMSCs.

RESULTS

BMMSCs express CBS/CSE and produce H₂S

Since H₂S plays important biological roles in a variety of cell types, we hypothesized that H₂S may affect BMMSC function. Interestingly, we found that both human and mouse BMMSCs expressed CBS and CSE, as assessed by Western blot, RT-PCR, and immunostaining (Figures 1A–1C). Double immunostaining showed that BMMSCs coexpressed CD73, a mesenchymal stem cell marker, with CBS and CSE (Figures 1D and 1E). BMMSCs were also able to produce H₂S in culture supernatant at a level of 8–10 μM, which was upregulated by the treatment of H₂S donor NaHS and downregulated by the treatment of the CBS inhibitor hydroxylamine (HA) or the CSE inhibitor D, L-propargylglycine (PAG) (Figure 1F and Figure S1A). However, combined treatment using HA and PAG showed the same H₂S reduction as observed in the groups that received only HA or PAG (Figure 1F). Moreover, we revealed that mouse serum H₂S levels were upregulated by intraperitoneal (IP) injection of NaHS and downregulated by IP injection of HA or PAG (Figure 1G). Combined injection of HA and PAG showed similar downregulated H₂S levels to ones observed in the HA or PAG groups (Figure 1G). These data indicate that BMMSCs express both CBS and CSE, and produce H₂S. H₂S production by BMMSCs is upregulated by H₂S donor and downregulated by H₂S inhibitor, respectively. In addition to expressing CBS and CSE, both human and mouse BMMSCs express 3-mercaptopyruvate sulfurtransferase (3-MST) and cysteine aminotransferase (CAT), as shown by Western blot, RT-PCR, immunocytostaining, and flow cytometric analysis (Figures S1B–S1F). When expression of either 3-MST or CAT was knocked down by siRNA, H₂S production by BMMSCs was partially reduced and their *in vitro* osteogenic differentiation was impaired, assessed by alizarin red staining (Figures S1G–S1I).

H₂S is required for maintenance of BMMSC function *in vivo*

To examine whether H₂S serves as a physiologic gasotransmitter to regulate stem cell properties, we used CBS knockout mice as an H₂S-deficient model to examine BMMSC function (Watanabe et al., 1995). Previous study showed that CBS knockout mice had a cartilage deficiency, but was not reported whether they also had osteogenic disorder (Watanabe et al., 1995). We revealed that CBS^{-/-} mice displayed several abnormalities, including severe growth retardation and developmental defects (Figure S2A), which led to death at 4 weeks of age in most cases (Watanabe et al., 1995). CBS^{+/-} mice survived normally, and only 1/50 mice showed the reduction in body weight and loose hair that were observed in CBS^{-/-} mice (Figure S2A). CBS protein was absent in CBS^{-/-} BMMSCs and decreased to half of normal levels in CBS^{+/-} BMMSCs (Figure S2B). Endogenous H₂S levels in serum showed a 50% reduction in both CBS^{-/-} and CBS^{+/-} mice compared with normal C57BL6 mice (Figure 2A), which may indicate production of H₂S using CSE as an alternative enzyme. Furthermore, we revealed that cultured CBS^{-/-} and CBS^{+/-} BMMSCs produced similarly reduced levels of H₂S (Figure 2B). All CBS^{-/-} mice and 66.6% of CBS^{+/-} mice had osteopenia phenotypes, as assessed by histological analysis that showed reduced femur trabecular bone volume (Figure 2C) and microCT analysis that showed reduced bone mineral density (BMD) and bone volume/tissue volume (BV/TV) in femurs (Figure 2D).

Since it is unknown whether CBS deficiency affects BMMSCs, we next revealed that CBS^{-/-} and CBS^{+/-} BMMSCs showed increased proliferation rates (Figures 2E). When cultured under osteo-inductive conditions, CBS^{-/-} and CBS^{+/-} BMMSCs showed reduced capacities for mineralized nodule formation, expression of the osteogenic makers Runx2-related transcription factor 2 (Runx2) and alkaline phosphatase (ALP), and regeneration of new bone when implanted into immunocompromised mice subcutaneously (Figures 2F and 2G). However, when induced under adipogenic conditions, CBS^{-/-} and CBS^{+/-} BMMSCs showed adipogenic differentiation capacities similar to that observed in normal BMMSCs, as assessed by Oil red O staining to show the number of adipocytes and RT-PCR to show expression levels of lipoprotein lipase (*LPL*) and peroxisome proliferator-activated receptor-gamma 2 (*PPAR* γ 2) (Figure S2C).

Interestingly, elevating H₂S levels in CBS^{+/-} BMMSCs by *in vitro* H₂S donor NaHS treatment was able to rescue their cell proliferation rate, capacity for mineralized nodule formation, expression of osteogenic markers Runx2 and ALP, and capacity for *in vivo* bone formation (Figures 3A–3C). However, H₂S donor NaHS treatment failed to affect adipogenic differentiation in CBS^{+/-} BMMSCs, as shown by Oil red O staining and RT-PCR to show expression levels of *LPL* and *PPAR* γ 2 (Figure S3A). These data imply that H₂S is required for maintaining stem cell properties of BMMSCs.

H₂S is required for maintenance of BMMSC function *in vitro*

We next used an *in vitro* culture system to examine the role of H₂S in BMMSC proliferation and differentiation. When treated with the CBS inhibitor HA, the CSE inhibitor PAG, CBS siRNA or CSE siRNA to reduce H₂S levels, BMMSCs showed a similar phenotype to the one observed in CBS^{+/-} BMMSCs, including increased proliferation rate, reduced capacity for forming mineralized nodules *in vitro*, downregulation of Runx2 and ALP, and reduced new bone formation when implanted into immunocompromised mice subcutaneously (Figures 3D–3F). In contrast, reducing H₂S levels in BMMSCs using CBS inhibitor, CSE inhibitor or CBS siRNA treatment showed no effect on their adipogenic differentiation (Figures S3B–S3D). These data confirm that H₂S is required to maintain BMMSC self-renewal and osteogenic differentiation.

Elevation of H₂S level in CBS^{+/-} mice rescues osteopenia phenotype and BMMSC function

In order to examine whether H₂S donor treatment rescues BMMSC function and osteopenia phenotype in H₂S-deficient mice, H₂S donor GYY4317 was IP injected into CBS^{+/-} mice every other day at 1 mg/mouse for 28 days (total of 14 injections) (Figure 4A). After the last injection, serum H₂S levels, femur trabecular bone volume, BMD, and BV/TV were significantly increased in CBS^{+/-} mice (Figures 4B–4D). Additionally, BMMSCs from GYY4317-treated CBS^{+/-} mice showed significant rescue of cell proliferation rate, capacity to form mineralized nodules, expression of the osteogenic markers Runx2 and ALP, and formation of new bone *in vivo* when compared to the untreated CBS^{+/-} BMMSCs (Figures 4E–4G). As expected, GYY4317 treatment failed to affect adipogenic differentiation of CBS^{+/-} BMMSCs, as evaluated by the number of Oil Red O-positive cells and expression levels of *LPL* and *PPAR* γ 2 (Figures S4A and S4B). These results indicate that elevation of

H₂S levels by H₂S donor treatment is capable of rescuing the osteopenia phenotype and osteogenic deficiency of BMMSCs in CBS^{+/-} mice.

CBS inhibitor HA and CSE inhibitor PAG treatment resulted in osteopenia phenotype and BMMSC impairment *in vivo*

Next, we examined whether injection of CBS inhibitor to reduce H₂S levels would cause osteopenia phenotype and BMMSC impairment, as observed in CBS^{+/-} mice. When CBS inhibitor HA was IP-injected into C57BL6 mice every other day at 100 µg/mouse for 28 days (totally 14 injections), serum H₂S levels and CBS protein expression levels were significantly decreased when compared to the untreated control group (Figures 5A–5C). HA treatment resulted in a significant reduction in femur trabecular bone area, BMD, and BV/TV in C57BL6 mice (Figures 5D and 5E). BMMSCs derived from HA-treated mice showed the same phenotype observed in CBS^{+/-} BMMSCs, including increased proliferation rate, decreased population doubling, decreased capacity to form mineralized nodules and expression of the osteogenic makers Runx2 and ALP, as well as reduced new bone formation *in vivo* (Figures 5F–5I). However, HA treatment failed to affect the adipogenic differentiation of BMMSCs (Figure 5J). These data suggest that reduction of H₂S levels may be directly associated with BMMSC impairment and osteopenia phenotype. Moreover, when CSE inhibitor PAG was IP injected into C57BL6 mice every other day at 100 µg/mouse for 28 days (a total of 14 injections) (Figure S5A), serum H₂S levels and CSE protein expression levels were significantly decreased when compared to the untreated control group (Figures S5B and S5C). PAG treatment resulted in a significant reduction in femur trabecular bone area, BMD, and BV/TV in C57BL6 mice (Figures S5D and S5E). BMMSCs derived from PAG-treated mice showed the same phenotype observed in CBS^{+/-} BMMSCs, including increased proliferation rate and decreased capacity to form mineralized nodules and expression of the osteogenic makers Runx2 and ALP, as well as reduced new bone formation *in vivo* (Figures S5F–S5H).

H₂S level, but not homocysteine accumulation, may contribute to BMMSC impairment in CBS-deficient mice

CBS deficiency-induced homocysteine accumulation may contribute to diseased phenotypes in CBS-deficient patients (Gaustadnes et al., 2000; Kelly et al., 2003; Kluijtmans et al., 1999; Maclean et al., 2002; Miles and Kraus, 2004). In order to clarify whether homocysteine accumulation affects BMMSC function in CBS-deficient conditions, we assessed plasma homocysteine levels in CBS deficient mice and found that CBS^{-/-} mice had 34 times greater plasma homocysteine levels than age-matched C57BL6 (WT) mice. However, CBS^{+/-} mice, which have an osteopenia phenotype similar to CBS^{-/-} mice, showed plasma homocysteine levels only twice as high as age-matched C57BL6WT mice (Figures S5I and S5J). Both CBS^{-/-} and CBS^{+/-} mice showed elevated numbers of tartrate-resistant acid phosphatase (TRAP) positive osteoclasts in their femurs and elevated receptor activator of nuclear factor kappa-B ligand (RANKL) levels in serum when compared to WT control mice. CBS^{-/-} mice, however, exhibited a more significant increase in the number of TRAP positive osteoclasts and higher levels of RANKL than that of CBS^{+/-} mice (Figures S5K and S5L). These data suggest that homocysteine levels may be associated with osteoclast activity. Although IP injection of H₂S donor GYY4317 rescued the osteopenia

phenotype and BMMSC function in CBS^{+/-} mice, it failed to reduce serum homocysteine levels in CBS^{+/-} mice (Figure S5M). These data suggest that H₂S levels may affect the osteopenia phenotype *via* regulating BMMSC differentiation in CBS-deficient mice. Although IP injection of CBS inhibitor reduced H₂S levels and resulted in an osteopenia phenotype in C57BL6 mice (Figures 5L and 5M), only slightly elevated serum homocysteine levels was observed (Figure S5N), confirming that H₂S levels affect the osteopenia phenotype. To determine whether homocysteine has any direct effect on BMMSCs, we used a dose of 100–200 μM homocysteine to treat BMMSCs *in vitro* and found that the treatment failed to affect cell proliferation, *in vitro* mineralized nodule formation, and *in vivo* bone formation of BMMSCs (Figures S5)-S5Q). This experimental evidence suggests that H₂S levels, but not homocysteine, may directly affect BMMSC function. In addition, we showed that *in vitro* NaHS treatment resulted in reduced numbers of osteoclasts, while homocysteine treatment increased osteoblast numbers (Figure S5R).

H₂S deficiency causes BMMSC impairment *via* attenuation of Ca²⁺ influx

H₂S serves as a gasotransmitter to control cellular Ca²⁺ levels, which, in turn, regulate cell biological signaling (Distrutti, 2011; Li et al., 2011; Ogawa et al, 2012). We showed that H₂S donor NaHS treatment induced a concentration-dependent Ca²⁺ influx in BMMSCs (Figure 6A). H₂S-induced Ca²⁺ elevation mainly resulted from Ca²⁺ influx with a limited contribution from intracellular Ca²⁺ storage (Figure 6B). Single TRP channel knockdown by siRNA for the TRPC subfamily (TRPC1, 3, and 7), TRPV subfamily (TRPV1 and 4) and TRPM subfamily (TRPM2, 4, and 8) failed to block H₂S-induced (NaHS 100 μM) Ca²⁺ influx in BMMSCs (Figures S6A–S6L). No significant difference was observed in the amount of Ca²⁺ influx among the different groups (Figure S6M). These data suggest that H₂S may affect not only one specific TRP Ca²⁺ channel, but rather multiple different TRP Ca²⁺ channels. Thus, we next tested the effect of combinations of siRNA knockdown of three TRP channels (TRPV6, TRPV3, and TRPM4) that contain cysteine (Cys) residues with potential to undergo sulfhydrylation. Interestingly, we found that knockdown of TRPV6, TRPV3, and TRPM4 together blocked more than 50% of H₂S-induced (NaHS 100 μM) Ca²⁺ influx in BMMSCs (Figure 6C). These results indicate that H₂S affects multiple TRPs channels that may be associated with Cys residue sulfhydrylation.

Sulfhydryl number in Ca²⁺ channels determines H₂S-induced Ca²⁺ influx

H₂S modifies specific Cys residues (–SH) in proteins through the formation of a persulfide (–SSH) bond, and this modification has been termed protein sulfhydrylation. The physiological function of sulfhydrylation may be involved in the regulation of inflammation and endoplasmic reticulum stress signaling, as well as vascular tension (Krishnan et al., 2011; Li et al., 2006). In order to further explore if H₂S levels affect Ca²⁺ channel sulfhydrylation in BMMSCs, the numbers of free Cys residues (sulfhydryl, –SH) on cytomembrane between H₂S-deficient and normal BMMSCs were compared using classical Ellman's reagent (Ellman, 1959). Free sulfhydryls were found in decreased numbers in CBS^{+/-} BMMSCs when compared to normal BMMSCs (Figure 6D). These data demonstrate that the number of free sulfhydryls in BMMSC membranes may correlate with H₂S-induced Ca²⁺ influx. Next, we used chemical agent treatment to alter the number of free sulfhydryls and measured if this treatment affected H₂S-induced Ca²⁺ influx.

Dithiothreitol (DTT) can reduce the disulfide bonds of proteins and increase the number of residual sulfhydryl proteins (Cleland, 1964). In contrast, diamide (DM) is capable of reducing the number of sulfhydryls (Kosower et al., 1969), and (2-sulfonatoethyl) methane thiosulfonate (MTSES) is a nonpermeable reagent able to reduce free sulfhydryls only on the outer cytomembrane (Chen et al., 1997). In comparison to the control group (Figure S6N), DTT-treated BMMSCs showed an elevated amount of NaHS-induced Ca^{2+} influx (Figure S6N). DM-treated BMMSCs showed a reduction in NaHS-induced Ca^{2+} influx (Figure S6N). MTSES treatment also decreased NaHS-induced Ca^{2+} influx in BMMSCs, but not as effectively as the DM treatment did (Figure S6N). Quantitative analysis confirmed that DTT treatment elevated levels of Ca^{2+} influx and free sulfhydryl in BMMSCs (Figures 6E and 6F). In contrast, DM and MTSES treatment induced reduced levels of Ca^{2+} influx and free sulfhydryl in BMMSCs (Figures 6E and 6F). These results suggest that the number of free sulfhydryls, both inside and outside of the BMMSC cytomembrane, affects NaHS-induced Ca^{2+} influx. We used 1 mM of DTT, DM and MTSES to treat BMMSCs for 15 minutes, which failed to affect cell viability (data not shown).

Sulfhydration (SHY) is a physiological process whereby H_2S attaches an additional sulfur to the sulfhydryl ($-\text{SH}$) groups of Cys yielding a hydropersulfide ($-\text{SSH}$) (Krishnan et al., 2011). In order to examine whether H_2S affects sulfhydration of Ca^{2+} TRP channels, we used a modified Alexa Fluor 488-conjugated C5 maleimide (green maleimide) assay to detect sulfhydration. Maleimide interacts selectively with sulfhydryl groups of Cys, labeling both sulfhydrated and unsulfhydrated Cys. An advantage of this method is that nitrosylated or oxidized Cys do not react with maleimide. The samples were treated with DTT, which selectively cleaves disulfide bonds and detaches the green signal from sulfhydrated protein, but not unsulfhydrated protein, resulting in decreased fluorescence. We employed green maleimide to detect transient receptor potential (TRP) sulfhydration in BMMSCs with or without H_2S treatment (Figure 6G). We first selected TRPV6 as a representative TRP protein to examine sulfhydration. The level of sulfhydration of TRPV6 was calculated based on the residual green fluorescence intensity compared to the total amount of TRPV6 protein, which was regulated by DTT treatment (Figure 6H). We found that without H_2S treatment, DTT did not affect the levels of “green” TRPV6 protein, indicating the absence of sulfhydration (Figure 6H). In contrast, H_2S treatment reduced the green signal in the presence of DTT, indicating that sulfhydration had occurred in the TRPV6 protein. We further employed mass spectrometric analysis to identify the Cys residue responsible for sulfhydration of TRPV6 proteins in BMMSCs. We used online LC-Orbitrap MS and CID MS/MS to confirm that H_2S treatment converted SH to SSH at specific modification sites (Figure S6O). The conversion leads to a defined mass change of the peptide from PDI digest, which was directly measured with a high level of confidence by high-resolution MS (Figure S6P). The mass shift suggested that BMMSCs were modified by H_2S through S-sulfhydration of Cys residues. Then we used CID fragmentation MS/MS to localize the modification sites with single amino acid resolution. Detection of precursor ions at high resolution and a nearly complete series of fragmentation ions from CID allowed the accurate sequencing and identification of a single site of modification. Integrating MS and CID MS/MS results, Protein Discoverer 1.3 automatically assigned potential modification sites

with a high level of confidence. After H₂S treatment, we found that Cys residues were sulfhydrated, with a high level of confidence, at the C172 and C329 sites (Figures S6O and S6P). Next, we generated TRPV6^{C172mu} and TRPV6^{C329mu} constructs and overexpressed TRPV6, TRPV6^{C172mu}, TRPV6^{C329mu} and TRPV6^{C172+C329mu} in BMMSCs (Figure S6Q and S6U). Overexpression of TRPV6 could slightly increase Ca²⁺ influx, and it activated Ca²⁺ downstream signaling p-PKC and active β-catenin, along with downregulation of p-Erk (Figures S6R and S6S). At the functional level, overexpression of TRPV6 in BMMSCs increased *in vitro* osteogenic differentiation (Figure S6T). Overexpression of TRPV6^{C172+C329mu}, but not TRPV6^{C172mu} or TRPV6^{C329mu}, reduced H₂S donor-induced upregulation of p-PKC and active β-catenin and *in vitro* osteogenic differentiation in the TRPV6 group (Figures S6S and S6T). These data suggest although H₂S affects sulfhydration in multiple Ca²⁺ channels, TRPV6 C172 and C329 contribute at least partially to sulfhydration-controlled Ca²⁺ influx in BMMSCs. In addition to TRPV6, we showed that other Ca²⁺ TRP channels, including TRPV3 and TRPM4, were also assigned sulfhydration sites with a high level of confidence at Cys residues *via* fluorescence Western blot and CID MS/MS (Figures S6V–S6X). These data suggest that multiple TRP Ca²⁺ channels are sulfhydrated after H₂S treatment.

Reduction of H₂S levels induced osteogenic deficiency in BMMSCs *via* Wnt/β-catenin pathway

In order to examine how H₂S deficiency-induced reduction of Ca²⁺influx affects osteogenic differentiation of BMMSCs, we analyzed three Ca²⁺ downstream pathways, including PCK/Erk, PI3K/Akt/GSK3β and CaMKII/Calcineurine A cascades, which are closely linked to Ca²⁺-associated regulation of osteogenic differentiation (Li et al., 2011; Lof et al., 2012). We found that expression levels of p-PKC significantly decreased along with upregulation of p-Erk in CBS^{+/-} BMMSCs and H₂S inhibitor-treated BMMSCs (Figure 7A). However, expression levels of PI3K/Akt and CaMKII showed no difference between CBS^{+/-} and control BMMSCs (Figure S7A). Therefore, we focused on assessing PCK/Erk signaling and confirmed that H₂S inhibitor-treated BMMSCs have decreased expression of p-PCK and elevated expression of p-Erk (Figure 7A). In contrast, H₂S donor NaHS treatment induced upregulation of p-PKC, but downregulation of p-ERK in BMMSCs (Figure 7A). NaHS treatment failed to upregulate p-PKC expression in BMMSCs (Figure 7B). Since Erk inhibitor treatment failed to affect p-PKC expression in BMMSCs (Figure 7C), Erkmight be downstream of the PKC pathway. Taken together, these data indicate that H₂S-regulated Ca²⁺ influx affects p-PKC and p-Erk expression in BMMSCs.

Since PKC phosphorylation can serve as part of the Wnt/calcium pathway, which regulates osteogenic differentiation of BMMSCs, we examined expression levels of total β-catenin and active β-catenin. We found that expression of β-catenin and active β-catenin was decreased in both CBS^{+/-} and H₂S inhibitor-treated BMMSCs (Figure 7D). Moreover, when TOPflash and its control FOPflash were transfected to normal and CBS^{+/-} BMMSCs, comparing the relative levels of luciferase activity confirmed that the canonical Wnt/β-catenin pathway was inhibited in CBS^{+/-} BMMSCs (Figure 7E). Reduced β-catenin levels in both CBS^{+/-} BMMSCs and H₂S inhibitor-treated BMMSCs were rescued by H₂S donor NaHS treatment, again as assessed by relative luciferase activity (Figure 7F). Interestingly,

PKC inhibitor treatment blocked NaHS-rescued β -catenin expression in both CBS^{+/-} and H₂S inhibitor-treated BMMSCs (Figure 7G), suggesting that the PCK pathway may regulate β -catenin expression under CBS-deficient conditions. Additionally, we showed that PKC activator and Erk inhibitor treatment rescued the osteogenic deficiency in CBS^{+/-} and H₂S inhibitor-treated BMMSCs, as assessed by alizarin red staining, Western blot analysis, and *in vivo* BMMSC implantation (Figures 7H–7J, Figure S7B). These data confirm that PCK and Erk pathways contribute to H₂S deficiency-associated osteogenesis. Moreover, combinative knockdown of sulfhydrylation-associated of Ca²⁺ channels TRPV6, TRPV3, and TRPM4, which reduced NaHS-induced Ca²⁺ influx (Figure 6C), also resulted in upregulation of P-Erk, along with downregulation of p-PKC and active- β -catenin (Figure 7K). Moreover, combinative knockdown of TRPV6, TRPV3, and TRPM4 in BMSMCs by siRNA resulted in reduced mineralized nodule formation and expression of osteocalcin and Runx2 (Figures S7C and S7D). NaHS treatment failed to rescue altered expression of p-Erk, p-PKC, and active- β -catenin, as assessed by Western blot (Figure 7L) and also failed to affect knockdown-induced mineralized nodule formation and expression of osteocalcin and Runx2 (Figures S7C and S7D), indicating that H₂S-induced Ca²⁺ influx in BMMSCs was regulated by multiple Ca²⁺ channels, at least including TRPV6, TRPV3, and TRPM4, *via* a sulfhydrylation manner.

DISCUSSION

Reduction of H₂S levels contributes to osteopenia phenotype in CBS-deficient mice

Classic clinical features of untreated CBS-deficient patients include a variety of phenotypes, including myopia, ectopia lentis, mental retardation, thromboembolic disorders, and osteoporosis. Osteoporosis is characterized by low bone mass and deterioration of osseous microarchitecture, resulting in decreased bone strength and increased risk of fragility fractures. This phenotype is often observed in patients with hyperhomocysteinemia (Herrmann et al., 2005; Melton, 2003). Cell culture studies have suggested that high homocysteine (HCY) levels may stimulate osteoclast activity (Herrmann et al., 2005; Koh et al., 2006). Our data showed that osteoclast activity was significantly increased in CBS deficient mice, in which both HCY and RANKL may enhance osteoclast activity. The effect of high HCY levels on osteoblasts is controversial. Increased concentrations of HCY may enhance cell apoptosis through activation of the NF- κ B pathway and impair osteogenic differentiation in osteoblast cell line HS-5 (Koh et al., 2006). Other reports showed that increased concentrations of HCY stimulate primary human osteoblast differentiation (Herrmann et al., 2007; Herrmann et al., 2008) and may not damage the osteogenic function of preosteoblastic cells (Carmel et al., 1988; Sakamoto et al., 2005; Thaler et al., 2010). In this study, we found that HCY treatment failed to induce BMMSC impairment. Although CBS^{-/-} mice showed an increase in serum HCY level to about 34 times that of controls, while the level in CBS^{+/-} mice only doubled, both CBS^{-/-} and CBS^{+/-} BMMSCs showed a marked impairment of osteogenic differentiation, along with an osteopenia phenotype. Therefore, we hypothesize that BMMSC impairment, which may not be related to the high level of HCY, also contributes to the osteopenia phenotype observed in CBS-deficient mice.

In addition to the elevated levels of HCY, a CBS-deficient condition results in a reduction in the H₂S level. However, it was unknown whether this reduced H₂S level contributes to the osteopenia phenotype. In this study, we revealed that elevating H₂S levels in CBS^{+/-} mice by H₂S donor GYY4317 treatment rescued the osteopenia phenotype, but failed to significantly alter the HCY level. In addition, CBS inhibitor treatment failed to significantly elevate the HCY level, but did result in an osteopenia phenotype like the one observed in CBS^{+/-} mice, with marked impairment of BMMSCs. Although intraperitoneal injection of CBS inhibitor HA only partially reduced the expression level of CBS, the same as observed in CBS^{+/-} mice, the HA treatment was capable of significant reducing the levels of H₂S. These data suggest that partial deficiency of CBS expression is capable of reducing H₂S levels, resulting in an osteopenia phenotype. The reduction of H₂S levels in the bone microenvironment plays a critical role in CBS deficiency-associated osteopenia, perhaps through regulation of BMMSC functions.

H₂S regulates Ca²⁺ influx via sulfhydration of TRP channels in BMMSCs

H₂S-induced Ca²⁺ influx was diminished in CBS-deficient BMMSCs and CBS inhibitor-treated BMMSCs, suggesting that the H₂S, at the physiological level, plays a critical role in maintaining normal function of the Ca²⁺ channels in BMMSCs. The mechanism underlying H₂S control of different Ca²⁺ channels is unknown. Interestingly, when the number of sulfhydryl groups on TRP channels was altered by DTT and DM treatment, H₂S-induced Ca²⁺ influx was significantly affected. These data suggest that the number of sulfhydryl groups in Cys of multiple TRP channels may regulate H₂S-mediated Ca²⁺ influx.

The unique function of a gasotransmitter, which differs from classical signaling molecules in the body, lies in its ability to permeate membranes freely and to target specific molecules easily. It has been widely accepted that a single ligand usually reacts with one special Ca²⁺ channel. Here, we suggest that a physiological level of H₂S maintains the sulfhydryl levels in order to ensure normal Ca²⁺ channel function. In the process of sulfhydration, the sulfhydryl group of a reactive Cys is modified to an -SSH group, resulting in increased reactivity of the Cys residue.

Conclusion

The functional role of H₂S in different tissues is still not fully elucidated. Our study indicates that physiological levels of H₂S are required to maintain intercellular Ca²⁺ homeostasis by sulfhydration of multiple TRP channels in BMMSCs. Reduction of H₂S levels results in a cascade response in BMMSCs, including altered Ca²⁺ channel sulfhydration, Ca²⁺ influx, Wnt/β-catenin signaling, and osteogenic differentiation. The eventual result is an osteoporosis phenotype. It is anticipated that advances in understanding the role of H₂S may lead to H₂S donor-based therapeutic approaches for H₂S deficiency-related disorders (Mancardi et al., 2009).

EXPERIMENTAL PROCEDURES

Animals

Female C57BL/6J and 129P2-*Cbs*^{tm1Unc}/J mice were purchased from the Jackson Lab (Bar Harbor, ME). Female immunocompromised mice (Beige *nude/nude* XIDIII) were purchased from Harlan (Indianapolis, IN). All animal experiments were performed under institutionally approved protocols for the use of animal research (University of Southern California protocols #10874 and 10941).

Isolation of mouse bone marrow mesenchymal stem cells (BMMSCs)

Bone marrow cells were flushed out from the bone cavities of femurs and tibias with 2% heat-inactivated fetal bovine serum (FBS; Equitech-Bio, Kerrville, TX) in PBS. Single-cell suspension of all nuclear cells (ANCs) was obtained by passing through 70 μm cell strainer (BD Bioscience, Franklin Lakes, NJ). All nuclear cells were seeded at 15×10^6 into 100 mm culture dishes (Corning Corporation) and initially incubated for 48 hours at 37 °C in 5% CO₂. To eliminate the nonadherent cells, the cultures were washed with PBS twice. The attached cells were cultured for 16 days. The BMMSCs were cultured with alpha minimum essential medium (Alpha-MEM, Invitrogen Corporation, Carlsbad, CA) supplemented with 20% FBS, 2 mM L-glutamine (Invitrogen Corporation), 55 μM 2-mercaptoethanol (Invitrogen Corporation), 100 U/ml penicillin, and 100 $\mu\text{g}/\text{ml}$ streptomycin (Invitrogen Corporation).

Injection of H₂S donor and inhibitor into mice

H₂S donor NaHS and GYY4317, CBS inhibitor HA, and CSE inhibitor PAG were intraperitoneally injected into mice, as described in Table S2. One month later, the samples were harvested, and further experiments were carried out.

Cytoimmunofluorescent microscopy

The cells were subcultured on 8-well chamber slides (Nunc) (2×10^3 /well) under the culture medium for 12 hours at 37°C in 5% CO₂. Then the samples were fixed in 4% paraformaldehyde, followed by 0.01% Triton-100 treatment for 10 min. The samples were blocked with normal serum matched to secondary antibodies and incubated with specific isotype-matched mouse antibodies (1:200) overnight at 4 °C. The samples were treated with Rhodamine/FITC-conjugated secondary antibodies (1:200, Jackson ImmunoResearch, West Grove, PA; Southern Biotechnology, Birmingham, AL) and were mounted by means of a vectashield mounting medium containing 4', 6-diamidino-2-phenylindole (DAPI) (Vector Laboratories, Burlingame, CA).

Sulfhydryl groups measured by Ellman's test

Ellman's Reagent (5,5'-dithio-bis-[2-nitrobenzoic acid] DTNB) is used to quantitate free (reduced) sulfhydryl groups (-SH) by comparing to a standard curve of a sulfhydryl-containing compound, such as cysteine. Alternatively, sulfhydryl groups can be assayed using the extinction coefficient of TNB ($14,150 \text{ M}^{-1} \text{ cm}^{-1}$ at 412 nm). Ellman's Reagent has provided a reliable method to measure reduced cysteines and other free sulfhydryls in

solution. DTNB reacted with a free sulfhydryl group to yield a mixed disulfide and 2-nitro-5-thiobenzoic acid (TNB). The target of DTNB in this reaction is the conjugate base (R—S⁻) of a free sulfhydryl group. Briefly, 4 mg DTNB was dissolved in 1 ml reaction buffer (0.1 M sodium phosphate, pH 8.0, containing 1 mM EDTA). A set of test tubes was prepared, each containing 50 µl of Ellman's reagent solution and 2.5 ml of reaction buffer. To analyze the sulfhydryl groups in living cells, 500 µl of Ellman's reagent solution was directly added into each well of the culture plate, mixed and incubated at room temperature for 15 minutes. Then the solution was collected and absorbance measured at 412 nm. Cysteine hydrochloride monohydrate was used as a reference standard.

Supplementary Material

Refer to Web version on PubMed Central for supplementary material.

Acknowledgments

This work was supported by grants from the National Institute of Dental and Craniofacial Research, National Institutes of Health, Department of Health and Human Services (R01DE017449 and R01 DE019932 to S.S.), from the National Natural Science Foundation of China (81222011 to Y.L.), and from Science and Technology Activities of Beijing Overseas Students Preferred Foundation (to Y.L.).

References

- Abe K, Kimura H. The possible role of hydrogen sulfide as an endogenous neuromodulator. *J Neurosci.* 1996; 16:1066–1071. [PubMed: 8558235]
- Bao L, Vlcek C, Paces V, Kraus JP. Identification and tissue distribution of human cystathionine beta-synthase mRNA isoforms. *Arch Biochem Biophys.* 1998; 350:95–103. [PubMed: 9466825]
- Bukovska G, Kery V, Kraus JP. Expression of human cystathionine beta-synthase in *Escherichia coli*: purification and characterization. *Protein Expr Purif.* 1994; 5:442–448. [PubMed: 7827502]
- Carmel R, Lau KH, Baylink DJ, Saxena S, Singer FR. Cobalamin and osteoblast-specific proteins. *N Engl J Med.* 1988; 319:70–75. [PubMed: 3260008]
- Chen S, Hartmann HA, Kirsch GE. Cysteine mapping in the ion selectivity and toxin binding region of the cardiac Na⁺ channel pore. *J Membr Biol.* 1997; 155:11–25. [PubMed: 9002421]
- Cleland WW. Dithiothreitol, a New Protective Reagent for Sh Groups. *Biochemistry.* 1964; 3:480–482. [PubMed: 14192894]
- Dhonukshe-Rutten RA, Pluijm SM, de Groot LC, Lips P, Smit JH, van Staveren WA. Homocysteine and vitamin B12 status relate to bone turnover markers, broadband ultrasound attenuation, and fractures in healthy elderly people. *J Bone Miner Res.* 2005; 20:921–929. [PubMed: 15883631]
- Distrutti E. Hydrogen sulphide and pain. *Inflamm Allergy Drug Targets.* 2011; 10:123–132. [PubMed: 21275898]
- Donovan LM, Moore MW, Gillombardo CB, Chai S, Strohl KP. Effects of hydrogen sulfide synthesis inhibitors on posthypoxic ventilatory behavior in the C57BL/6J mouse. *Respiration.* 2011; 82:522–529. [PubMed: 21952225]
- Ellman GL. Tissue sulfhydryl groups. *Arch Biochem Biophys.* 1959; 82:70–77. [PubMed: 13650640]
- Erickson PF, Maxwell IH, Su LJ, Baumann M, Glode LM. Sequence of cDNA for rat cystathionine gamma-lyase and comparison of deduced amino acid sequence with related *Escherichia coli* enzymes. *Biochem J.* 1990; 269:335–340. [PubMed: 2201285]
- Fiorucci S, Antonelli E, Mencarelli A, Orlandi S, Renga B, Rizzo G, Distrutti E, Shah V, Morelli A. The third gas: H₂S regulates perfusion pressure in both the isolated and perfused normal rat liver and in cirrhosis. *Hepatology.* 2005; 42:539–548. [PubMed: 16108046]

- Friedenstein AJ, Chailakhyan RK, Latsinik NV, Panasyuk AF, Keiliss-Borok IV. Stromal cells responsible for transferring the microenvironment of the hemopoietic tissues. Cloning in vitro and retransplantation in vivo. *Transplantation*. 1974; 17:331–340. [PubMed: 4150881]
- Gaustadnes M, Rudiger N, Rasmussen K, Ingerslev J. Intermediate and severe hyperhomocysteinemia with thrombosis: a study of genetic determinants. *Thromb Haemost*. 2000; 83:554–558. [PubMed: 10780316]
- Gil V, Gallego D, Jimenez M. Effects of inhibitors of hydrogen sulphide synthesis on rat colonic motility. *Br J Pharmacol*. 2011; 164:485–498. [PubMed: 21486289]
- Gjesdal CG, Vollset SE, Ueland PM, Refsum H, Meyer HE, Tell GS. Plasma homocysteine, folate, and vitamin B 12 and the risk of hip fracture: the hordaland homocysteine study. *J Bone Miner Res*. 2007; 22:747–756. [PubMed: 17295607]
- Herrmann M, Umanskaya N, Wildemann B, Colaianni G, Schmidt J, Widmann T, Zallone A, Herrmann W. Accumulation of homocysteine by decreasing concentrations of folate, vitamin B12 and B6 does not influence the activity of human osteoblasts in vitro. *Clin Chim Acta*. 2007; 384:129–134. [PubMed: 17673193]
- Herrmann M, Umanskaya N, Wildemann B, Colaianni G, Widmann T, Zallone A, Herrmann W. Stimulation of osteoblast activity by homocysteine. *J Cell Mol Med*. 2008; 12:1205–1210. [PubMed: 18782184]
- Herrmann M, Widmann T, Colaianni G, Colucci S, Zallone A, Herrmann W. Increased osteoclast activity in the presence of increased homocysteine concentrations. *Clin Chem*. 2005; 51:2348–2353. [PubMed: 16195358]
- Kelly PJ, Furie KL, Kistler JP, Barron M, Picard EH, Mandell R, Shih VE. Stroke in young patients with hyperhomocysteinemia due to cystathionine beta-synthase deficiency. *Neurology*. 2003; 60:275–279. [PubMed: 12552044]
- Kluijtmans LA, Boers GH, Kraus JP, van den Heuvel LP, Cruysberg JR, Trijbels FJ, Blom HJ. The molecular basis of cystathionine beta-synthase deficiency in Dutch patients with homocystinuria: effect of CBS genotype on biochemical and clinical phenotype and on response to treatment. *Am J Hum Genet*. 1999; 65:59–67. [PubMed: 10364517]
- Koh JM, Lee YS, Kim YS, Kim DJ, Kim HH, Park JY, Lee KU, Kim GS. Homocysteine enhances bone resorption by stimulation of osteoclast formation and activity through increased intracellular ROS generation. *J Bone Miner Res*. 2006; 21:1003–1011. [PubMed: 16813521]
- Kosower NS, Kosower EM, Wertheim B, Correa WS. Diamide, a new reagent for the intracellular oxidation of glutathione to the disulfide. *Biochem Biophys Res Commun*. 1969; 37:593–596. [PubMed: 5353890]
- Krishnan N, Fu C, Pappin DJ, Tonks NK. H₂S-Induced sulfhydration of the phosphatase PTP1B and its role in the endoplasmic reticulum stress response. *Sci Signal*. 2011; 4:ra86. [PubMed: 22169477]
- Li L, Bhatia M, Moore PK. Hydrogen sulphide--a novel mediator of inflammation? *Curr Opin Pharmacol*. 2006; 6:125–129. [PubMed: 16487749]
- Li L, Bhatia M, Zhu YZ, Zhu YC, Ramnath RD, Wang ZJ, Anuar FB, Whiteman M, Salto-Tellez M, Moore PK. Hydrogen sulfide is a novel mediator of lipopolysaccharide-induced inflammation in the mouse. *FASEB J*. 2005; 19:1196–1198. [PubMed: 15863703]
- Li L, Rose P, Moore PK. Hydrogen sulfide and cell signaling. *Annu Rev Pharmacol Toxicol*. 2011; 51:169–187. [PubMed: 21210746]
- Lof C, Sukumaran P, Viitanen T, Vainio M, Kemppainen K, Pulli I, Nasman J, Kukkonen JP, Tornquist K. Communication Between the Calcium and cAMP Pathways Regulate the Expression of the TSH Receptor: TRPC2 in the Center of Action. *Mol Endocrinol*. 2012; 26:2046–2057. [PubMed: 23015753]
- Macleane KN, Gaustadnes M, Oliveriusova J, Janosik M, Kraus E, Kozich V, Kery V, Skovby F, Rudiger N, Ingerslev J, et al. High homocysteine and thrombosis without connective tissue disorders are associated with a novel class of cystathionine beta-synthase (CBS) mutations. *Hum Mutat*. 2002; 19:641–655. [PubMed: 12007221]

- Mancardi D, Penna C, Merlino A, Del Soldato P, Wink DA, Pagliaro P. Physiological and pharmacological features of the novel gasotransmitter: hydrogen sulfide. *Biochim Biophys Acta*. 2009; 1787:864–872. [PubMed: 19285949]
- McLean RR, Jacques PF, Selhub J, Tucker KL, Samelson EJ, Broe KE, Hannan MT, Cupples LA, Kiel DP. Homocysteine as a predictive factor for hip fracture in older persons. *N Engl J Med*. 2004; 350:2042–2049. [PubMed: 15141042]
- Melton LJ 3rd. Adverse outcomes of osteoporotic fractures in the general population. *J Bone Miner Res*. 2003; 18:1139–1141. [PubMed: 12817771]
- Miles EW, Kraus JP. Cystathionine beta-synthase: structure, function, regulation, and location of homocystinuria-causing mutations. *J Biol Chem*. 2004; 279:29871–29874. [PubMed: 15087459]
- Ogawa H, Takahashi K, Miura S, Imagawa T, Saito S, Tominaga M, Ohta T. H₂S functions as a nociceptive messenger through transient receptor potential ankyrin 1 (TRPA1) activation. *Neuroscience*. 2012; 218:335–343. [PubMed: 22641084]
- Olson KR, Donald JA. Nervous control of circulation--the role of gasotransmitters, NO, CO, and H₂S. *Acta Histochem*. 2009; 111:244–256. [PubMed: 19128825]
- Pittenger MF, Mackay AM, Beck SC, Jaiswal RK, Douglas R, Mosca JD, Moorman MA, Simonetti DW, Craig S, Marshak DR. Multilineage potential of adult human mesenchymal stem cells. *Science*. 1999; 284:143–147. [PubMed: 10102814]
- Prockop DJ. Marrow stromal cells as stem cells for nonhematopoietic tissues. *Science*. 1997; 276:71–74. [PubMed: 9082988]
- Sakamoto W, Isomura H, Fujie K, Deyama Y, Kato A, Nishihira J, Izumi H. Homocysteine attenuates the expression of osteocalcin but enhances osteopontin in MC3T3-E1 preosteoblastic cells. *Biochim Biophys Acta*. 2005; 1740:12–16. [PubMed: 15878736]
- Simpson RC, Freedland RA. Factors affecting the rate of gluconeogenesis from L-cysteine in the perfused rat liver. *J Nutr*. 1976; 106:1272–1278. [PubMed: 956911]
- Stipanuk MH, Beck PW. Characterization of the enzymic capacity for cysteine desulphhydration in liver and kidney of the rat. *Biochem J*. 1982; 206:267–277. [PubMed: 7150244]
- Swaroop M, Bradley K, Ohura T, Tahara T, Roper MD, Rosenberg LE, Kraus JP. Rat cystathionine beta-synthase. Gene organization and alternative splicing. *J Biol Chem*. 1992; 267:11455–11461. [PubMed: 1597473]
- Tang C, Li X, Du J. Hydrogen sulfide as a new endogenous gaseous transmitter in the cardiovascular system. *Curr Vasc Pharmacol*. 2006; 4:17–22. [PubMed: 16472173]
- Thaler R, Spitzer S, Rumpler M, Fratzl-Zelman N, Klaushofer K, Paschalis EP, Varga F. Differential effects of homocysteine and beta aminopropionitrile on preosteoblastic MC3T3-E1 cells. *Bone*. 2010; 46:703–709. [PubMed: 19895920]
- Uren JR, Ragin R, Chaykovsky M. Modulation of cysteine metabolism in mice--effects of propargylglycine and L-cyst(e)ine-degrading enzymes. *Biochem Pharmacol*. 1978; 27:2807–2814. [PubMed: 736976]
- van Meurs JB, Dhonukshe-Rutten RA, Pluijm SM, van der Klift M, de Jonge R, Lindemans J, de Groot LC, Hofman A, Witteman JC, van Leeuwen JP, et al. Homocysteine levels and the risk of osteoporotic fracture. *N Engl J Med*. 2004; 350:2033–2041. [PubMed: 15141041]
- Wang R. Two's company, three's a crowd: can H₂S be the third endogenous gaseous transmitter? *FASEB J*. 2002; 16:1792–1798. [PubMed: 12409322]
- Wang R. The gasotransmitter role of hydrogen sulfide. *Antioxid Redox Signal*. 2003; 5:493–501. [PubMed: 13678538]
- Watanabe M, Osada J, Aratani Y, Kluckman K, Reddick R, Malinow MR, Maeda N. Mice deficient in cystathionine beta-synthase: animal models for mild and severe homocyst(e)inemia. *Proc Natl Acad Sci U S A*. 1995; 92:1585–1589. [PubMed: 7878023]
- Yusuf M, Kwong Huat BT, Hsu A, Whiteman M, Bhatia M, Moore PK. Streptozotocin-induced diabetes in the rat is associated with enhanced tissue hydrogen sulfide biosynthesis. *Biochem Biophys Res Commun*. 2005; 333:1146–1152. [PubMed: 15967410]
- Zhong G, Chen F, Cheng Y, Tang C, Du J. The role of hydrogen sulfide generation in the pathogenesis of hypertension in rats induced by inhibition of nitric oxide synthase. *J Hypertens*. 2003; 21:1879–1885. [PubMed: 14508194]

Highlights

- H₂S produced by mesenchymal stem cells (MSCs) regulates their osteogenic potential
- Loss of H₂S signaling causes osteoporotic phenotypes in mice
- H₂S deficiency reduces Ca²⁺ flux and sulfhydration of TRP Ca²⁺ channels
- Reduced intracellular Ca²⁺ flux reduces β-catenin activity *via* a PKC/Erk pathway

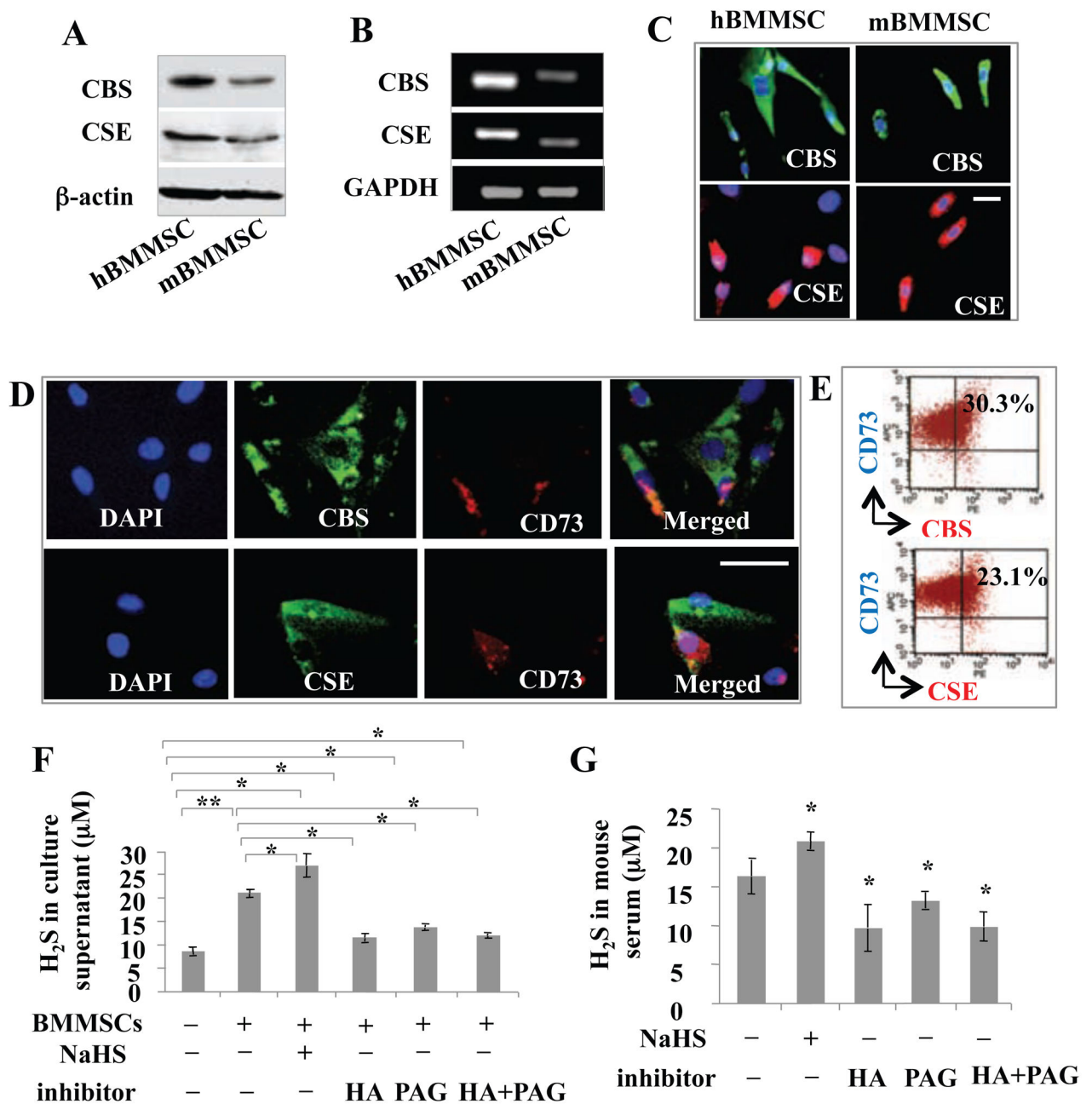


Figure 1. BMMSCs produced H₂S

(A, B) Both human (h) and mouse (m) BMMSCs express CBS and CSE, as assessed by Western blotting (A) and RT-PCR (B). (C) Immunocytochemical staining confirmed that both human and mouse BMMSCs expressed CBS and CSE. (D, E) Double immunostaining (D) and flow cytometric analysis (E) showed that 30% of CBS-positive and 23% of CSE-positive mouse BMMSCs expressed mesenchymal stem cell marker CD73. (F) Mouse BMMSC culture supernatant contained around 20 μM H₂S. H₂S levels were immediately upregulated by H₂S donor NaHS (100 μM) treatment and downregulated by CBS inhibitor hydroxylamine (HA, 100 μM) or CSE inhibitor D, L-propargylglycine (PAG, 100 μM)

treatment for 24 hours. When same amount of HA and PAG were added to the culture, the reduction of H₂S levels were the same as HA and PAG group. (G) The normal H₂S level in C57BL6 mouse serum is about 16.2 μM. H₂S levels were immediately elevated upon IP injection of H₂S donor NaHS and reduced by IP injection of CBS inhibitor HA or CSE inhibitor PAG treatment for 24 hours. Combinative IP injection of the same amount of HA and PAG showed the same levels of H₂S reduction as observed in HA and PAG group. * $P < 0.05$, ** $P < 0.01$, scale bar: 50 μm. Experiments were repeated three times. See also Figure S1.

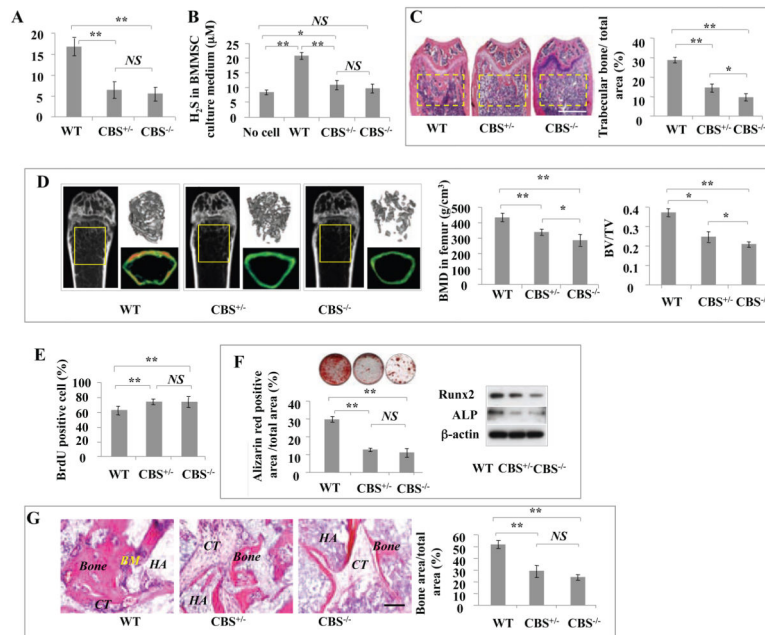


Figure 2. H₂S-deficient mice showed osteopenia phenotype and BMMSC impairment
(A) Serum H₂S levels decreased by almost half in CBS^{+/-} mice compared with control C57BL6 mice (WT). Although serum H₂S levels in CBS^{-/-} mice were lower than in CBS^{+/-} mice, no significant difference was observed between CBS^{+/-} and CBS^{-/-} mice. **(B)** H₂S levels in the culture supernatant of CBS^{+/-} and CBS^{-/-} BMMSCs showed a reduction to half that of the normal BMMSC group (WT). No cell: background control. **(C)** Femur trabecular bone volume in 66.6% of CBS^{+/-} mice and all CBS^{-/-} mice was significantly reduced (yellow square) in comparison to C57BL6 mice (WT), as evaluated by H&E staining analysis. **(D)** Osteopenia phenotype was confirmed in CBS^{+/-} and CBS^{-/-} mice by microQCT analysis. CBS^{+/-} and CBS^{-/-} mice showed significantly reduced bone mineral density (BMD) and bone volume/tissue volume (BV/TV) compared to C57BL6 mice (WT). **(E)** BrdU labeling assay showed that CBS^{+/-} and CBS^{-/-} BMMSCs had increased proliferation rates when compared to normal BMMSCs (WT). **(F)** When cultured under osteogenic inductive conditions, CBS^{+/-} and CBS^{-/-} BMMSCs showed reduced capacities to form mineralized nodules (evaluated by alizarin red staining) and express osteogenic markers Runx2 and ALP (evaluated by Western blotting). **(G)** When BMMSCs were subcutaneously implanted into immunocompromised mice using hydroxyapatite tricalcium phosphate (HA/TCP; HA) as a carrier, new bone regeneration was reduced in CBS^{+/-} and CBS^{-/-} BMMSC implants compared to normal BMMSC implants (WT). CT: connective tissue. **P*<0.05, ***P*<0.01, scale bar: 1000 µm (C), 200 µm (G). Experiments were repeated three times. See also Figure S2.

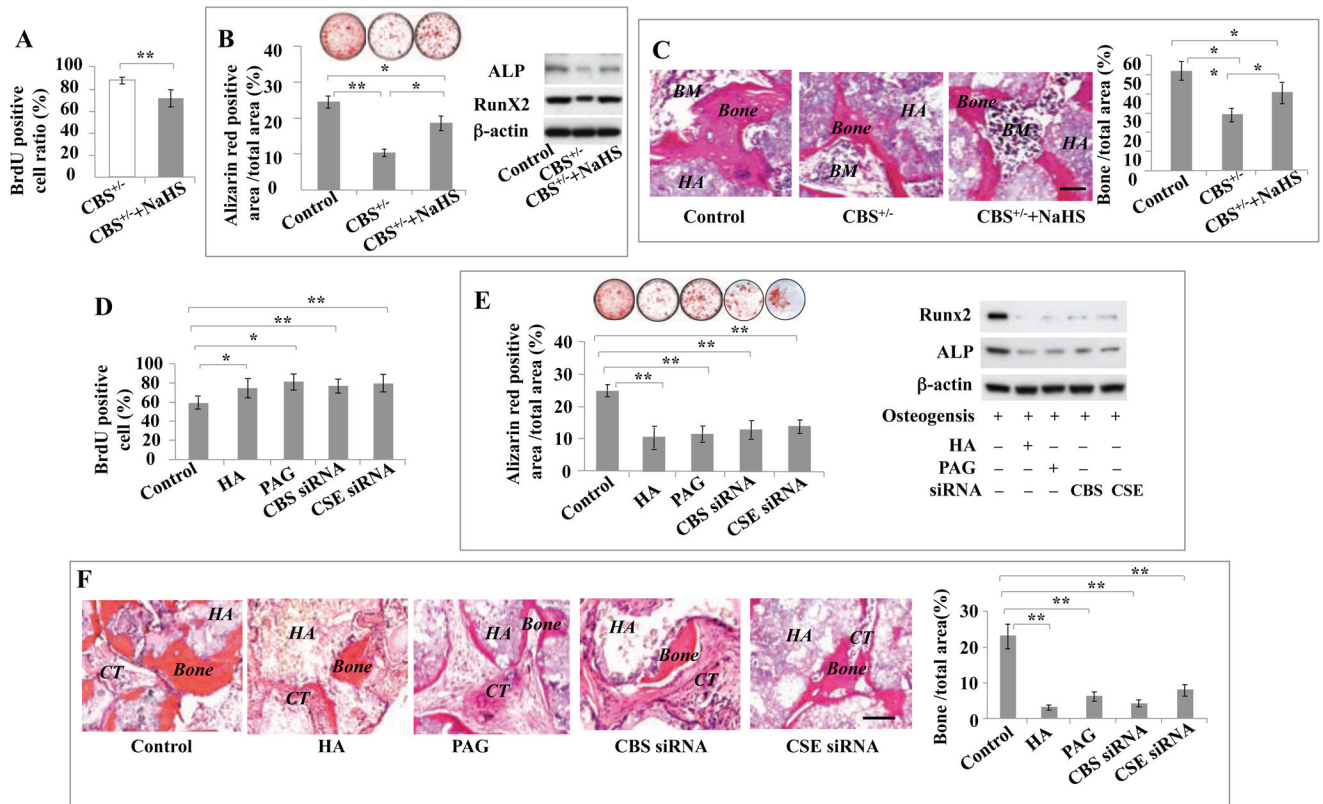


Figure 3. H₂S levels affected BMMSC function *in vitro*

(A, B) H₂S donor NaHS (100 μM) treatment for 24 hours rescued impaired CBS^{+/-} BMMSCs (CBS^{+/-}) function, as indicated by reduction of proliferation rate evaluated by BrdU staining (A) and elevation of mineralized nodule formation evaluated by alizarin red staining, and increased expression of osteogenic marker Runx2 and ALP evaluated by Western blotting (B). (C) When implanted into immunocompromised mice subcutaneously using HA/TCP (HA) as a carrier, NaHS-treated CBS^{+/-} BMMSCs (CBS^{+/-}+NaHS) showed improved capacity to generate new bone and bone marrow (BM). Normal BMMSCs were used as a control. (D–F) Moreover, we showed that blockage of H₂S levels by CBS inhibitor (HA, 100 μM), CSE inhibitor (PAG, 100 μM), CBS siRNA, and CSE siRNA treatment for 24 hours resulted in increased proliferation rate as evaluated by BrdU staining (D), but reduced mineralized nodule formation as shown by alizarin red staining, and reduced expression of osteogenic markers Runx2 and ALP as shown by Western blotting (E). Normal BMMSCs were used as a control. (F) When implanted into immunocompromised mice subcutaneously using HA/TCP (HA) as a carrier, BMMSCs treated by HA, PAG, CBS siRNA, or CSE siRNA showed reduction in the capacity to generate new bone *in vivo*. CT: connective tissue. * *P*<0.05, ** *P*< 0.01, scale bar: 200 μm. Experiments were repeated three times. See also Figure S3.

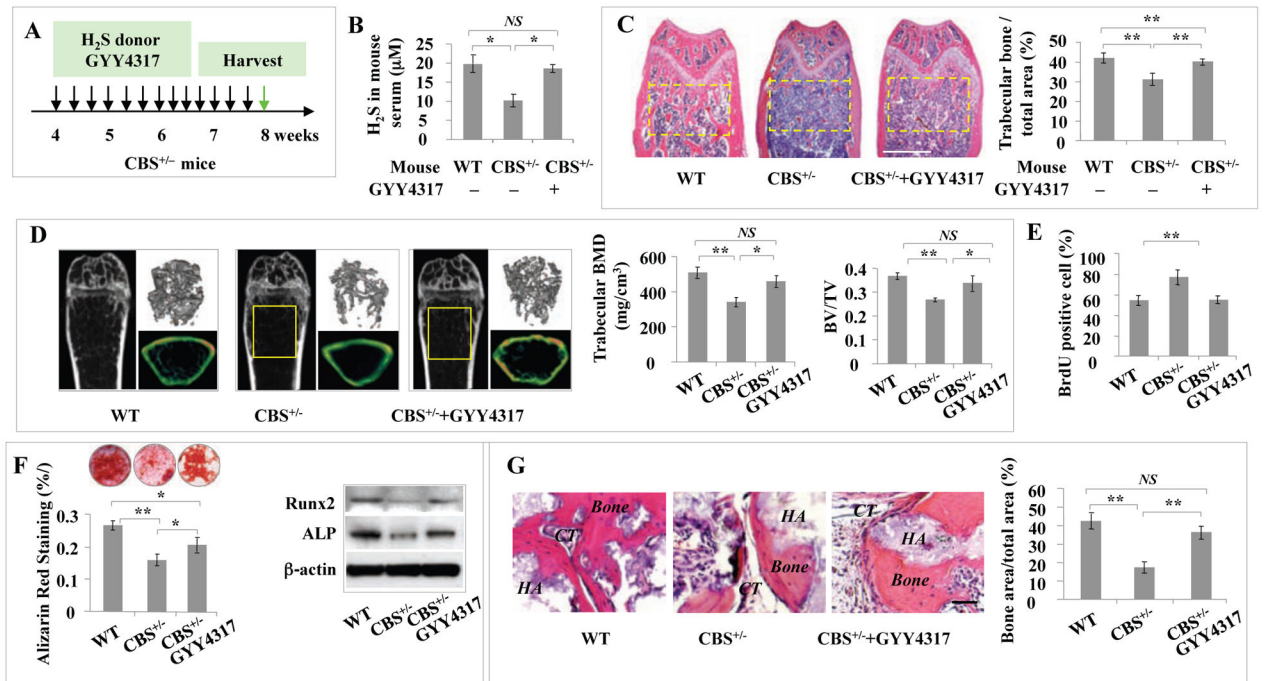


Figure 4. Intraperitoneal injection of H₂S donor GYY4317 rescued osteopenia phenotype and BMMSC function in CBS^{+/-} mice

(A) H₂S donor GYY4317 was IP injected to CBS^{+/-} mice every other day at 1 mg/mouse for 28 days (total 14 times). After the last injection, the samples were harvested for further experiments. (B–D) After GYY4317 treatment, CBS^{+/-} mice showed significantly increased serum H₂S levels (B), femur trabecular bone volume as shown by H&E staining (C), bone mineral density (BMD) and bone volume/tissue volume (BV/TV) as shown by microQCT (D). Wildtype mice were used as control (WT). (E–G) When compared with CBS^{+/-} BMMSCs (CBS^{+/-}), BMMSCs from GYY4317-treated CBS^{+/-} mice (CBS^{+/-} +GYY4317) showed reduced proliferation as evaluated by BrdU labeling (E), elevated mineralized nodule formation shown by alizarin red staining, elevated expression of osteogenic markers Runx2 and ALP (F), and increased new bone formation when implanted into immunocompromised mice subcutaneously using HA/TCP as a carrier (HA). CT: connective tissue (G). Wildtype mice were used as control (WT). * $P < 0.05$, ** $P < 0.01$, scale bar: 1000 μm (C), 200 μm (H). Experiments were repeated three times. See also Figure S4.

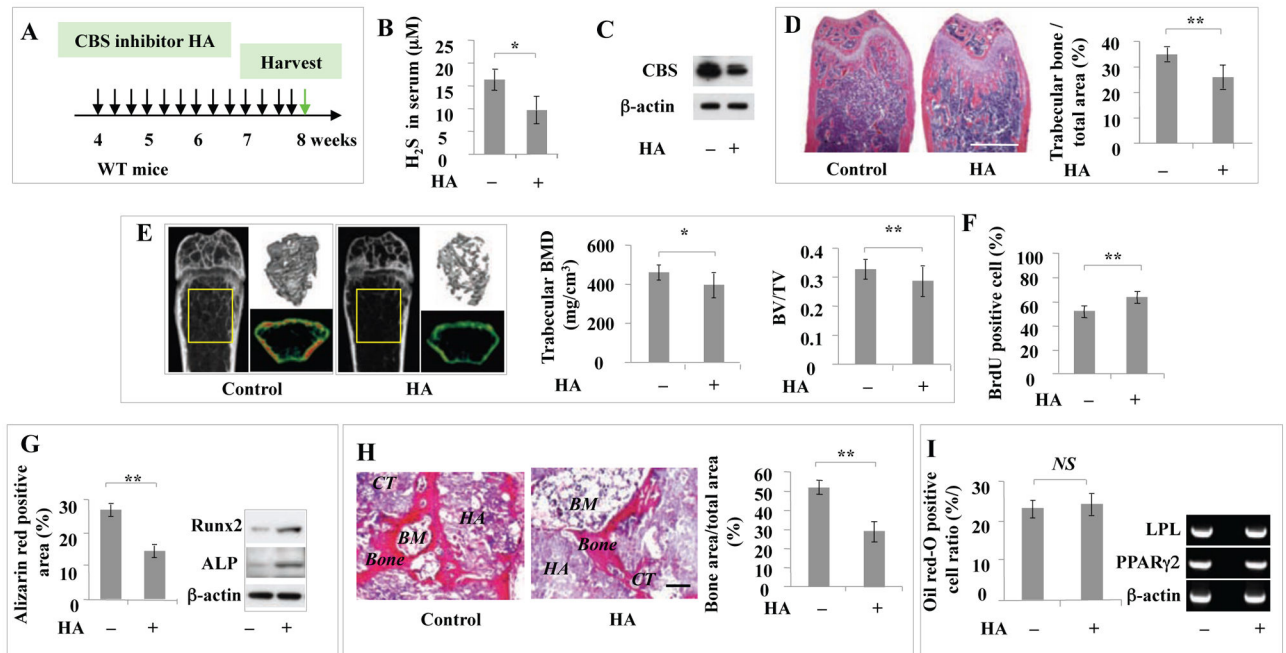


Figure 5. Intra-peritoneal injection of CBS inhibitor induced osteopenia phenotype and BMMSC impairment

(A) CBS inhibitor HA was IP injected to C57BL/6 mice every other day at 100 $\mu\text{g}/\text{mouse}$ for 28 days (totally 14 times injection), and after that BMMSCs were isolated. (B, C) HA injection resulted in significantly reduced levels of H_2S (B) and expression of CBS, as assessed by Western blotting (C). (D, E) HA injection induced marked reduction in mouse femur trabecular bone volume as assessed by H&E staining (D) and bone mineral density (BMD), as well as bone volume/tissue volume (BV/TV), as assessed by microQCT analysis (E). (F, G) BMMSCs derived from HA-treated mice showed increased proliferation rates, as assessed by BrdU labeling (F) and increased mineralized nodule formation as shown by alizarin red staining and increased expression of osteogenic markers Runx2 and ALP as shown by Western blotting (G). (H) BMMSCs from HA-treated mice showed decreased capacity to generate new bone when implanted into immunocompromised mice subcutaneously using HA/TCP (HA) as a carrier. BM: bone marrow; CT: connective tissue. (I) BMMSCs from HA-treated mice showed no change in the number of Oil red O-positive cells or expression of *LPL* and *PPAR γ 2* when compared to untreated control group. * $P < 0.05$, ** $P < 0.01$, scale bar: 1000 μm (D), 200 μm (I). Experiments were repeated three times. See also Figure S5.

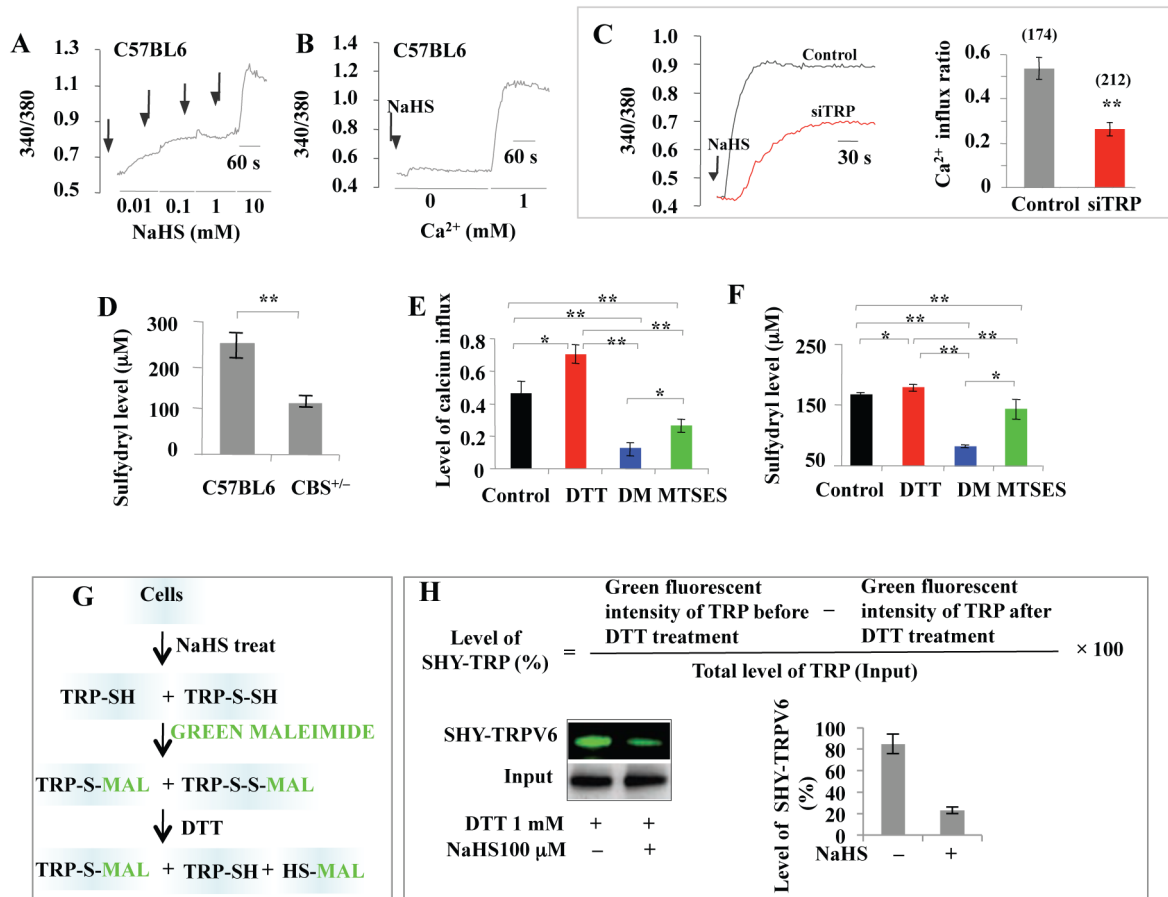


Figure 6. H₂S regulated Ca²⁺ influx via sulfhydration of Ca²⁺ channels

(A) Ca²⁺ levels were measured from the ratio of emission in response to excitation at 340 nm and 380 nm by microscopy. H₂S donor NaHS (10 μM to 10 mM) induced a dose-dependent Ca²⁺ influx in BMMSCs. Arrows represent the time points when H₂S donor NaHS was added. (B) When 100 μM NaHS, with or without 1 mM CaCl₂, was used to treat BMMSCs, Ca²⁺ flux only occurred in the presence of CaCl₂, indicating that the calcium influx mainly came from outside the cell membrane, but not from the endoplasmic reticulum or mitochondria. (C) When combination knockdown of TRPV6, TRPV3, and TRPM4 expression was induced in BMMSCs by siRNA, NaHS-induced Ca²⁺ flux was significantly reduced. (D) Ellman's test showed that sulfhydryl numbers on the cytomembrane were decreased in CBS^{+/-} BMMSCs when compared to normal BMMSCs. (E) Statistical analysis showed that 1 mM DTT treatment significantly elevated NaHS-induced Ca²⁺ influx, but 1 mM DM or MTSES significantly reduced NaHS-induced Ca²⁺ influx when compared to the control group (100 μM NaHS treatment). DM treatment exhibited more effective inhibition of Ca²⁺ influx than MTSES. (F) Ellman's test showed DTT treatment increased the number of free sulfhydryls in BMMSCs, while DM decreased the number of free sulfhydryls in BMMSCs. MTSES also reduced the sulfhydryl number in the BMMSC membrane. (G) Protein sulfhydration in BMMSCs, with or without NaHS treatment, was assessed by Alexa Fluor 488-conjugated C5 maleimide. (H) After 1 mM DTT treatment, sulfhydration of TRPV6 protein was calculated based on residual green fluorescence intensity in comparison

to total level of TRPV6 protein. Without NaHS treatment, DTT failed to affect the levels of “green” TRPV6 protein, indicating the absence of sulfhydration. In contrast, NaHS treatment reduced the green signal of TRPV6 protein in the presence of DTT, indicating that sulfhydration occurred. * $P < 0.05$, ** $P < 0.01$. Experiments were repeated three times. See also Figure S6.

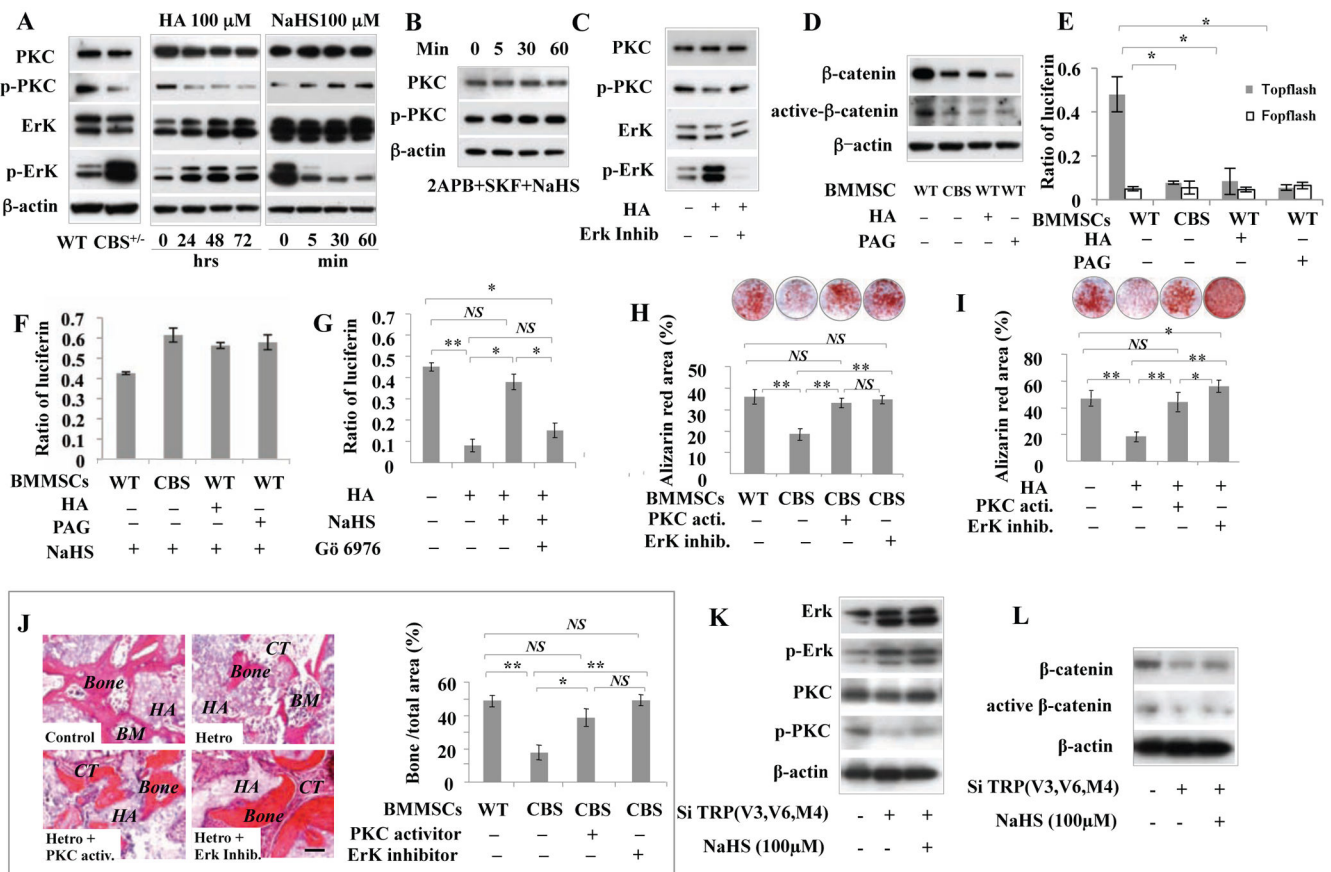


Figure 7. H₂S-deficiency downregulated Wnt/β-catenin pathway via reduced Ca²⁺ influx in BMMSCs

(A) CBS^{+/-} and H₂S inhibitor HA (100 μM)-treated BMMSCs cultured for 24, 48, or 72 hours showed significant downregulation of p-PKC and upregulation of p-Erk. In contrast, H₂S donor NaHS (100 μM) treatment for 5, 30, or 60 minutes upregulated p-PKC and downregulated p-Erk in BMMSCs. (B) When pretreated with 2APB (10 μM) and SKF-96365 (10 μM) for 15 min to block Ca²⁺ influx, NaHS treatment failed to upregulate p-PKC expression in BMMSCs. (C) Erk inhibitor (PD325901 1 μM) treatment failed to affect p-PKC expression in BMMSCs, indicating that Erk might be the downstream the PKC signaling. (D) When CBS inhibitor HA (100 μM) or CSE inhibitor PAG (100 μM) was used to reduce H₂S levels, BMMSCs showed significant reduction in total β-catenin and active β-catenin expression at 3 days post-treatment. (E) When TOPflash and control FOPflash were transfected into normal and CBS^{+/-} BMMSCs, luciferase activity indicated that the canonical Wnt/β-catenin pathway was inhibited in CBS^{+/-} BMMSCs in comparison to normal BMMSCs. (F) Reduced β-catenin expression in both CBS^{+/-} and H₂S inhibitor HA (100 μM)-treated BMMSCs was rescued by H₂S donor NaHS (100 μM) treatment, as assessed by luciferase activity. (G) Rescue of β-catenin expression by NaHS (100 μM) in both CBS^{+/-} and HA (100 μM)-treated BMMSCs was blocked by PKC inhibitor (Gö 6976, 10 nM) treatment, as assessed by luciferase activity. (H, I) PKC activator and Erk inhibitor treatment rescued the osteogenic deficiency in both CBS^{+/-} and HA-treated BMMSCs, as assessed by alizarin red staining to show mineral nodule formation. (J) *In vivo* BMMSC

implantation showed that PKC activator and Erk inhibitor treatment rescued CBS^{+/-} BMMSC-mediated new bone formation. *HA*: HA/TCP; *BM*: bone marrow; *CT*: connective tissue. **(K)** Western blotting showed that combinative knockdown of TRPV6, TRPV3, and TRPM4 channels by siRNA led to upregulation of p-Erk and downregulation of p-PKC, active- β -catenin and β -catenin. **(L)** H₂S donor NaHS treatment failed to rescue the altered expression of p-Erk, p-PKC, active- β -catenin and β -catenin, as assessed by Western blotting. * $P < 0.05$, ** $P < 0.01$. Experiments were repeated three times. See also Figure S7.